ACS Macro Letters

Letter

Cite This: ACS Macro Lett. 2019, 8, 1200−1208

pubs.acs.org/macroletters

pH-Responsive Micellar Nanoassemblies from Water-Soluble Telechelic Homopolymers Endcoding Acid-Labile Middle-Chain Groups in Their Hydrophobic Sequence-Defined Initiator Residue

Adrian Moreno,[†] Juan C. Ronda,[†] Virginia Cádiz,[†] Marina Galià,[†] Gerard Lligadas,*[,†,‡] and Virgil Percec*[,‡]

[†]Laboratory of Sustainable Polymers, Department of Analytical Chemistry and Organic Chemistry, University Rovira i Virgili, Tarragona 43007, Spain

[‡]Roy and Diana Vagelos Laboratories, Department of Chemistry, University of Pennsylvania, Philadelphia, Pennsylvania 19104-6323, United States

Supporting Information

ABSTRACT: A middle-chain cleavable telechelic poly(oligoethylene glycol) methyl ether acrylate) (MCCT-POEGA-Br) was synthesized by single-electron transfer living radical polymerization (SET-LRP) initiated from an acetal-containing hydrophobic sequence-defined difunctional initiator. In aqueous medium, above a certain concentration, this hydrophilic homopolymer self-assembled into nanogel-like large micelles that exhibit an encapsulating capacity for both hydrophobic and hydrophilic cargo. The sequence-defined cleavage pattern encoded in the initiator residue allowed precise middle-chain cleavage, leading to quantitative disassembly of the corresponding nanoobjects. Dye release studies performed in an acidic environment demonstrated the potential of this new design concept in the preparation of pH-responsive nanocarriers. In addition, fluorescently tagged nanoassemblies could also be obtained via the thio-bromo "click" modification of MCCT-POEGA-Br prior to self-assembly. This strategy may provide facile access to a diversity of multistimuli-responsive nanocarriers based on commercially available hydrophilic monomers and sequence-defined difunctional initiators synthesized by this simple design strategy.

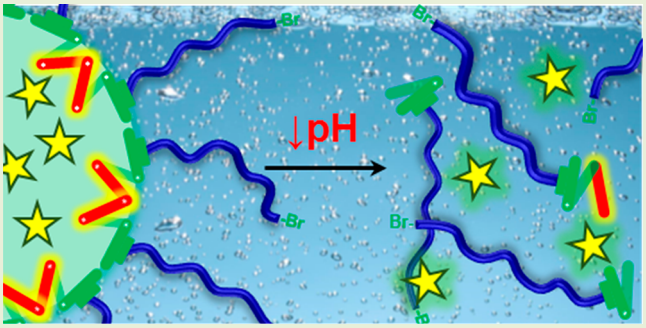

Supramolecular nanoscale systems based on amphiphilic block copolymers orchestrate important applications for nanofabrication, catalysis, and biomedicine.[1,2] An essential advantage of some of these advanced materials is the possibility to precisely control their disassembly processes in a spatiotemporal fashion. To this end, stimuli-responsive polymeric supramolecular assemblies integrating "sense and act" degradation, by a rational cleavage function, have aroused great interest.[3−6] In general, these nanoassemblies can be designed based on a myriad of functional groups able to sense external stimuli, including pH,[7] light,[8] enzymes,[9] and gases,[10] and to immediately undergo dramatic chemical structural changes. This feature allows controlled supramolecular disassembly, which is suitable to release encapsulated payloads for target delivery. Among the many activating signals exploited, pH triggers have a particular biological relevance because there are a wide range of pH gradients that exist in both biological and physiological systems.[11,12] In this context, cleavable polymers based on acetal linkages have attracted significant attention.[13−15]

Mimicking advanced and complex amphiphilic block copolymers, both neutral and zwitterionic amphiphilic homopolymers are also capable to self-assemble into well-defined nanostructures (e.g., nano/micro-particles,[16] hollow spheres,[17] and vesicles,[18]), making them promising materials for applications in drug delivery and nanotechnology.[19,20] In general, this special class of amphiphiles are prepared directly by living radical polymerization (LRP) of amphiphilic monomer[21−25] or via postpolymerization modification of a precursor polymer with selected hydrophilic and hydrophobic functionalities.[26−28] Surprisingly, the formation of high-order nanostructures can also be driven by the presence of one[29−33] or two[34−36] residual initiator hydrophobic end-groups in hydrophilic homopolymers prepared by LRP. Despite the fact that the latter approach is potentially simpler and more cost-effective because the use of commercially available hydrophilic monomers is common, research regarding the development of stimuli-responsive amphiphilic homopolymers so far remain somewhat limited to homopolymer-based synthetic monomers encoded with amphiphilic properties.[23,24,28] Thus, the

Received: July 25, 2019
Accepted: August 29, 2019
Published: September 3, 2019

DOI: 10.1021/acsmacrolett.9b00572
ACS Macro Lett. 2019, 8, 1200−1208

Scheme 1. General Concept Design for the Synthesis, Sequence-Defined Initiator Residue-Driven Micellar Assembly, and Disassembly of a Middle-Chain Cleavage Telechelic Homopolymers Prepared by LRP of Hydrophilic Monomers Initiated from Hydrophobic and Cleavable Difunctional Initiators[a]

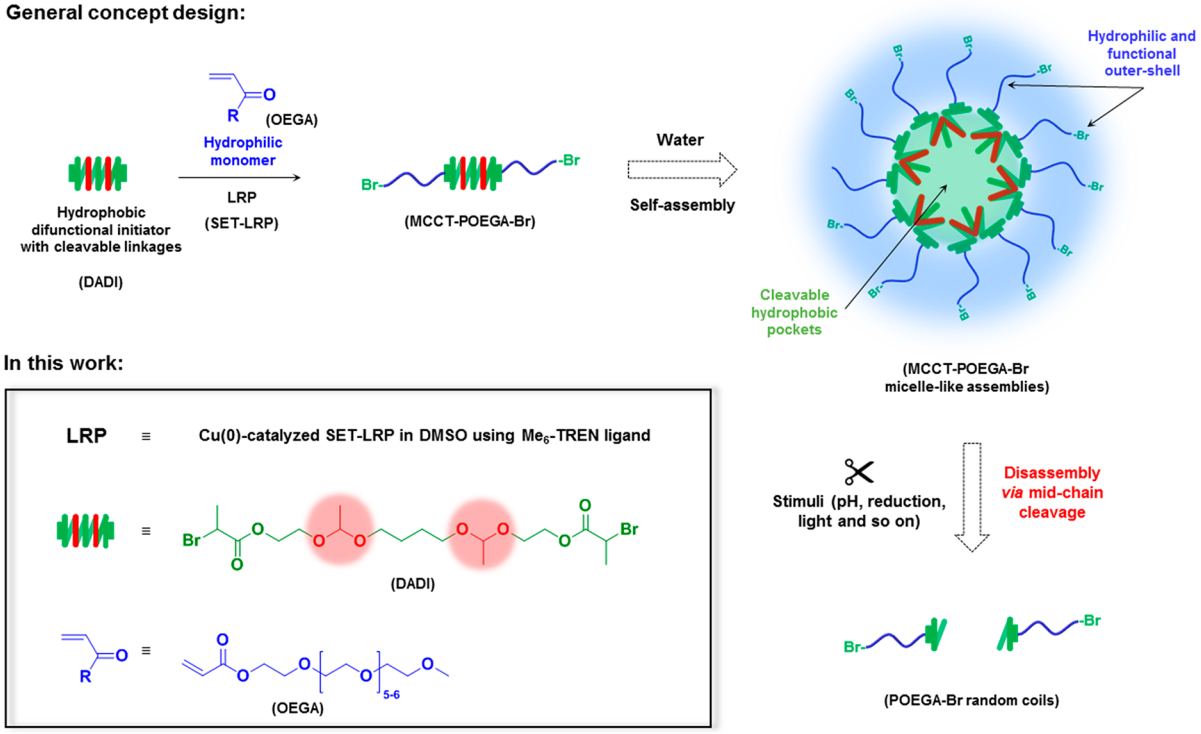

[a]Color code: blue as hydrophilic and water-soluble, green as hydrophobic and water insoluble, and red as labile linkage.

preparation of efficient and more accessible smart homopolymer responsive assemblies remains still a challenge. In this context, we envisaged that the LRP of hydrophilic monomers initiated from hydrophobic cleavable difunctional initiators can provide a facile access to stimuli-responsive micelle-like assemblies via midchain initiator residue-driven micellar assembly and subsequent disassembly via midchain initiator residue-cleavage (Scheme 1). This idea was inspired by the previously reported observations that hydrophilic oligo(ethylene oxide) methyl ether-derived monomers and initiators self-assemble in water into micellar aggregate structures[37] and the unusual self-assembly behavior of hydrophilic polymers containing both bulky and tiny hydrophobic residual initiator end groups.[34,29−31,35,32,36]

For proof of concept, this work focused on a telechelic homopolymer prepared by single-electron transfer living radical polymerization (SET-LRP)[38−42] from the hydrophobic α-haloester-type double acetal sequence-defined difunctional initiator (DADI)[43] and oligo(ethylene glycol) methyl ether acrylate (OEGA, M_n = 480 g mol^{-1}) as hydrophilic monomer (see inset in Scheme 1). The originality of the DADI relies mainly on the combination of hydrophobicity, flexibility, and precise cleavage pattern due to the presence of two acidic pH-sensitive midchain acetal linkages organized in a sequence-defined arrangement. To our knowledge, this is the first example of stimuli-responsive associative telechelic homopolymer encoded with cleavable middle-chain groups organized by the sequence-defined structure of the initiator. Detailed synthetic procedures regarding the synthesis of DADI and its use to initiate SET-LRP have been reported in a recent publication.[43] The homopolymers resulted from the SET-LRP of OEGA initiated with DADI may resemble an ABA triblock copolymer with a short central hydrophobic segment. However, it is incorrect to consider these homopolymers as ABA triblock copolymers since the DADI initiator is a monodisperse sequence-defined hydrophobic initiator containing two very precisely incorporated acid-cleavable groups.[44−46]

This sequence was never incorporated previously in homopolymers and demonstrated to behave as a block copolymer although it is a homopolymer and it would not even be of interest to be transformed into broad molecular weight distribution homopolymers generated by a step condensation polymerization process. Therefore, while examples of related structures based on ABA triblock copolymers are available in the literature,[1,2] the experiment reported here is unprecedented.

Kinetic studies previously demonstrated that Cu(0)-catalyzed SET-LRP of methyl acrylate (MA) from DADI and other related cleavable difunctional initiators is living in both homogeneous and "programmed" biphasic reaction mixtures.[42] A detailed GPC and MALDI-TOF analysis was used to prove that the use of DADI enables the discrete insertion of two labile midchain acetal groups into poly(MA) (PMA), thus, allowing a subsequent reduction of the molar mass of the corresponding polymer by half via acid-catalyzed acetal hydrolysis under mild conditions (Figure S1). Based on these encouraging results, telechelic poly(OEGA) (MCCT-POEGA-Br) was synthesized from DADI at a targeted degree of polymerization (DP) of 20 by SET-LRP at 25 °C using Cu(0) wire, tris[2-(dimethylamino)ethyl]amine (Me_6-TREN), and DMSO as catalyst, ligand, and disproportionating solvent, respectively (Scheme 1). As expected, polymerization was fast

DOI: 10.1021/acsmacrolett.9b00572
ACS Macro Lett. 2019, 8, 1200−1208

and reached almost quantitative monomer conversion (>94%) after 30 min. ^{1}H NMR analysis of purified MCCT-POEGA-Br confirmed the incorporation of the DADI-derived sequence-defined initiator residue at the midpoint of the telechelic polymer (Figure 1, middle spectrum). The bromine chain-end

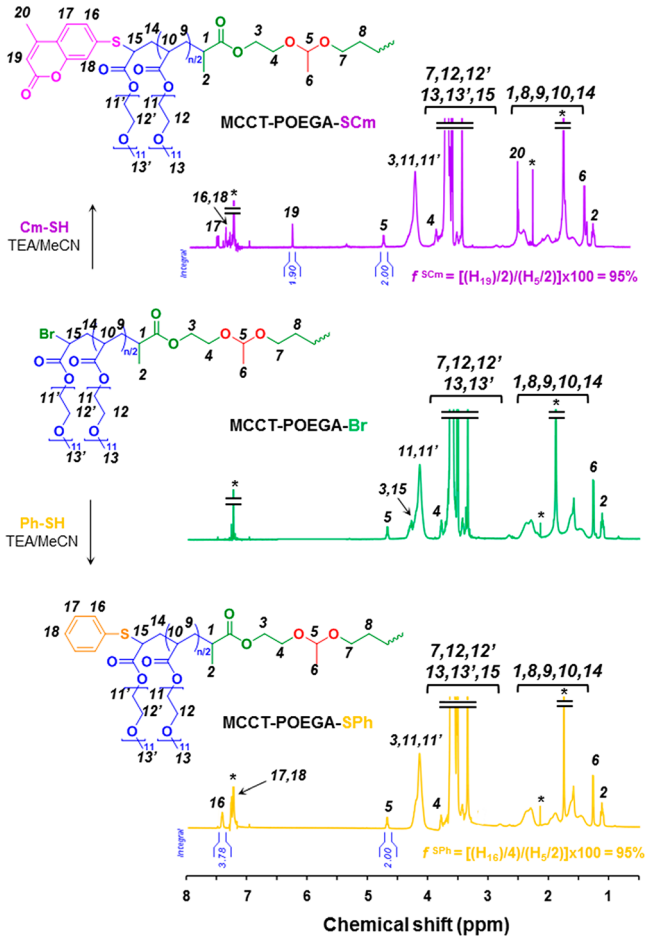

Figure 1. ^{1}H NMR spectra of middle-chain cleavable telechelic MCCT-POEGA-Br before (green trace) and after the thio-bromo "click" thioetherification of both end-groups with thiophenol (MCCT-POEGA-SPh, purple trace) and 3-mercaptocoumarin (MCCT-POEGA-SCm, orange trace) in the presence of TEA in MeCN. ^{1}H NMR resonances from residual nondeuterated solvents are indicated with *.

fidelity of the synthesized polymer could only be determined indirectly, after the thio-bromo "click" thioetherification derivatization reaction with thiophenol leading to MCCT-POEGA-SPh, due the overlapping of end-group signals with those of the polymeric chain (Figure 1, lower spectrum).[47,48]

The high degree of functionality (f > 95% at 96% conversion) is consistent with previous reports from our and other laboratories[49−51] and undoubtedly offers appealing reactive centers for potential applications (vide infra). GPC analysis in THF indicated that MCCT-POEGA-Br is well-defined (M_n^{GPC} = 9400, M_w/M_n = 1.21), although it revealed the presence of a small shoulder peak at a relatively high molecular weight region,[52,53] which may be indicative of a very small extent of bimolecular termination occurring at near complete conversion (Figure S2a).[37]

To test our design hypothesis, we analyzed the self-assembly and aggregation of MCCT-POEGA-Br in aqueous solution via direct dissolution. Due to the small hydrophobic fraction as low as 3 wt % in this hydrophilic polymer, it was not surprising that a transparent solution to visible light was obtained when water was added to MCCT-POEGA-Br at concentration of 1 mg·mL^{-1} (Figure 2a). However, we were gratified to observe that MCCT-POEGA-Br solutions showed increasing turbidity when the concentration exceeded 5 mg·mL^{-1}, presumably due to self-association of the telechelic polymer to form larger aggregates in water. We hypothesize that the folded chain structure of the obtained telechelic polymer might be the dominant conformation in MCCT-POEGA-Br nanoassemblies (see Scheme 1). As a control, the behavior of an analogous homopolymer BPE-POEGA-Br, also prepared by SET-LRP from conventional bis(2-bromopropionyl)ethane (BPE) difunctional initiator under strictly identical reaction conditions, was compared to the above results. The chemical structure and GPC analysis of this homopolymer are shown in Figures S3 and S2b, respectively. The fact that an aqueous solution of BPE-POEGA-Br at high concentration (20 mg mL^{-1}) appeared clear as pure water pointed out the special self-assembling abilities of the DADI-derived homopolymer (Figure 2a). To confirm the above empirical observations and gain further insight into the key role of DADI-derived hydrophobic and sequence-defined initiator residue in promoting self-assembly, we performed concentration-dependent dynamic light scattering (DLS), transmission electron microscopy (TEM), and ^{1}H NMR (in D_2O) measurements. The first series of DLS measurements was performed in methanol in order to evaluate the average hydrodynamic diameter (D_h) of both polymers in a random coil conformation. The analysis at various concentrations revealed the presence of BPE-POEGA-Br and MCCT-POEGA-Br unimers (D_h ∼ 3−5 nm; Figure S4). According to the above-discussed digital images, DLS analysis of the control homopolymer showed the same pattern after switching methanol by pure water, thus, suggesting a random coil conformation in both solvents (Figure S5). Accordingly, the ^{1}H NMR spectra of BPE-POEGA-Br measured in $CDCl_3$ and D_2O did not show significant differences in terms of intensity (Figure S6). However, MCCT-POEGA-Br self-organized in pure water at concentration of 1 mg·mL^{-1} into nearly monodisperse aggregates with D_h of approximately 100 nm and polydispersity (PDI) of 0.195 (Figure 2b). Importantly, the order of magnitude obtained for this hydrophilic homopolymer in aqueous solution does not correspond to simple polymeric micellar assemblies with common core−shell morphology.[54,55] High-resolution TEM visualization confirmed the presence spherical shape nanoassemblies with much smaller particle sizes than that measured by DLS (Figure 2c,d). Polymer nanostructures prepared at higher concentration were also well-defined, although aggregate size increased steadily with increase of polymer concentration (Figure 2b). However, in all cases, the particle size distribution averaged by intensity, volume, and number was monomodal and consistent (see Figure S7 as a representative example). In light of these results, the MCCT-POEGA-Br assemblies are thought to be nanogel-like large compound micelles (LCMs; see schematic representation in Figure 2e).[54−56] For these LCMs, attractive interactions favor the interaction and overlapping of poly(OEGA) chains and drives the aggregation of simple sphere-like micelles.[57] Consequently, the core of the LCMs self-assembled from MCCT-POEGA-Br contains many hydrophobic domains interconnected by hydrophilic islands

DOI: 10.1021/acsmacrolett.9b00572
ACS Macro Lett. 2019, 8, 1200−1208

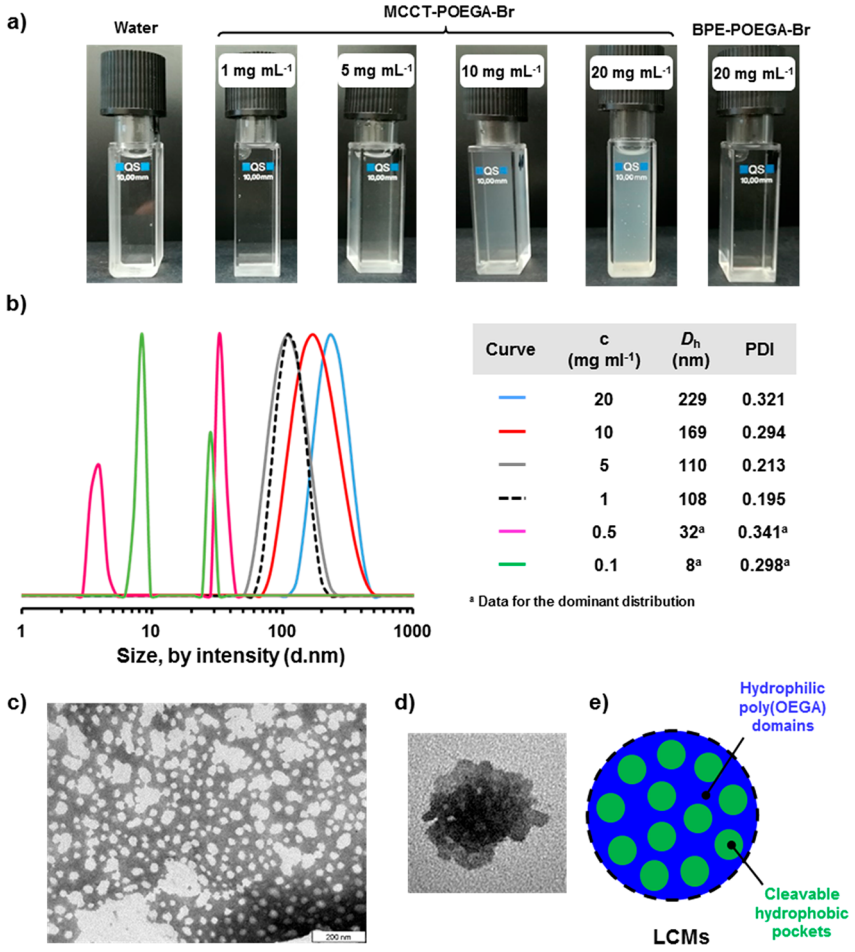

Figure 2. (a) Digital images of water, aqueous solutions of MCCT-POEGA-Br nanoassemblies at various concentrations and BPE-POEGA-Br at 20 mg·mL^{-1}. (b) DLS measurements and data of MCCT-POEGA-Br nanoassemblies in aqueous solution. (c, d) Representative TEM images with negative staining using phosphotungstic acid and a discrete nonstained nanoassembly showing aggregated morphology and (e) proposed schematic representation of LCMs self-assembled from MCCT-POEGA-Br at 1 mg·mL^{-1}.

based on loose poly(OEGA) chains. In this line, the ^{1}H NMR signals of poly(OEGA) chains appeared much more attenuated when the spectrum was recorded in D_2O than in $CDCl_3$ (at the same concentration; Figure S8). Indeed, due to deep penetration of water into these particles, such morphologies showed an important difference in particle size as measured from TEM than DLS.

Obviously, such interchain interactions are highly concentration dependent. Hence, when concentration of MCCT-POEGA-Br was decreased to 0.5 mg·mL^{-1}, DLS analysis revealed the transition from LCMs to common polymer micelles ($D_h \sim 30$ nm) coexisting with pure unimers ($D_h \sim 4$ nm; Figure 2b). DLS analysis at 0.1 mg·mL^{-1} showing a higher presence of unimers suggests that there must be a concentration where the hydrophilic telechelic homopolymer is water-soluble. Overall, these results point out that the presence of a hydrophobic and flexible SET-LRP initiator midchain residue is a fundamental requirement to formulate such nanoassemblies prepared from only one monomer and a difunctional initiator.

Next, we were interested in the loading capabilities and pH-responsiveness of MCCT-POEGA-Br LCMs for potential applications as nanocarriers. Nile red (NR) was used as a model payload to investigate the encapsulating capacity of the hydrophobic domains within the LCMs core (Figure 3a). As such, NR is poorly soluble in water as can be discerned from its emission spectrum in such solvent (Figure 3b, dashed red line). However, in the presence of MCCT-POEGA-Br (1 mg mL^{-1}), it became soluble, and the corresponding solution showed a characteristic emission peak at 625 nm (red line). The NR loading content in the LCMs was determined to be around 6.1% by UV spectroscopy using a standard curve. This result confirms that the reported LCMs are able to sequester NR in water. The sensibility of NR emission to the polarity of the microenvironment was then used to determine the critical aggregation concentration (CAC) of the LCMs (Figure 3c). While a negligible change in fluorescence intensity was detected at low concentrations of MCCT-POEGA-Br indicating that few nanoassemblies are present, a dramatic increase was noticed at higher concentrations of amphiphilic homopolymer. This suggests that NR is located in the hydrophobic pockets of LCMs assemblies. Thus, the relationship between fluorescence intensity and logarithm of polymer concentration is nonlinear, and the onset point corresponds to the CAC. The low CAC value (0.72 mg L^{-1}) indicates good stability of these nanoobjects in future applications. Inspired by previous reports,[56] we also investigated the ability of LCM aggregates to encapsulate hydrophilic guest molecules inside the hydrophilic domains of such nanoassemblies (Figure 3a). Calcein is a hydrophilic fluorescent dye that shows a clear peak in the

DOI: 10.1021/acsmacrolett.9b00572
ACS Macro Lett. 2019, 8, 1200−1208

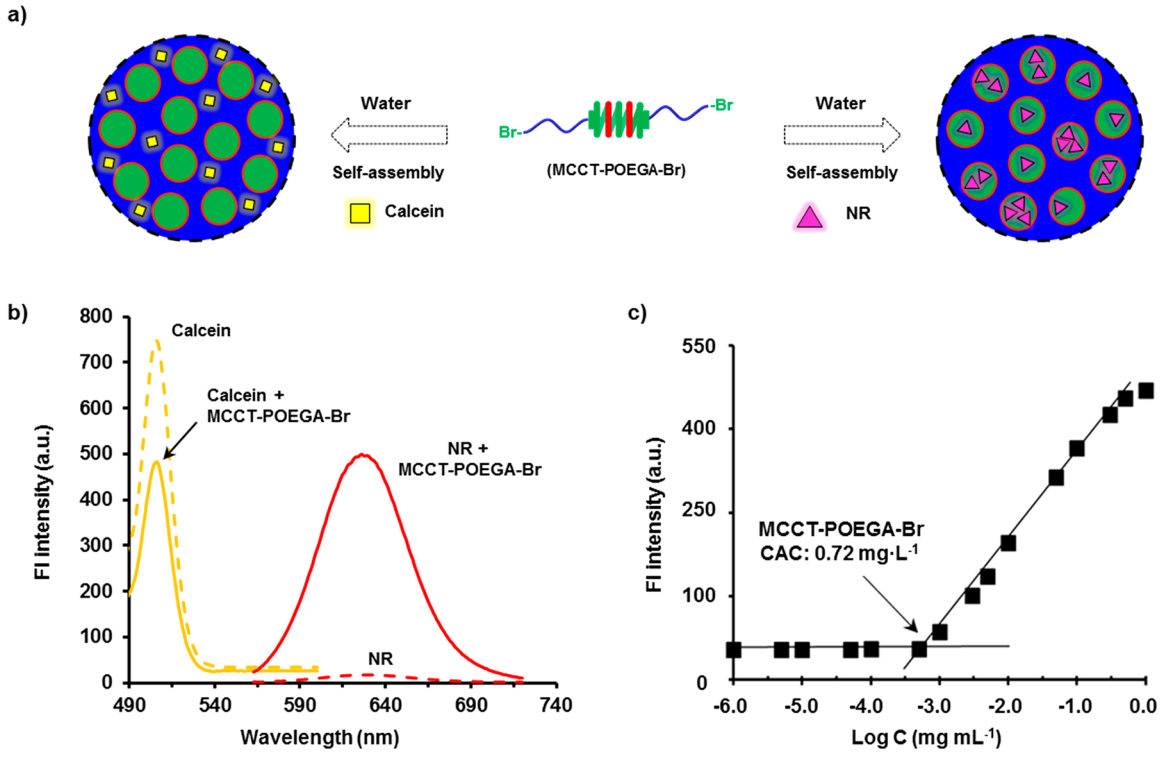

Figure 3. (a) Schematic representation of self-assembly of MCCT-POEGA-Br with calcein and NR encapsulation. (b) Emission spectrum of NR and calcein in water and aqueous solution of MCCT-POEGA-Br. (c) Fluorescence intensity of NR at 625 nm (λ_{exc} = 550 nm) vs MCCT-POEGA-Br concentration (mg·mL^{-1}).

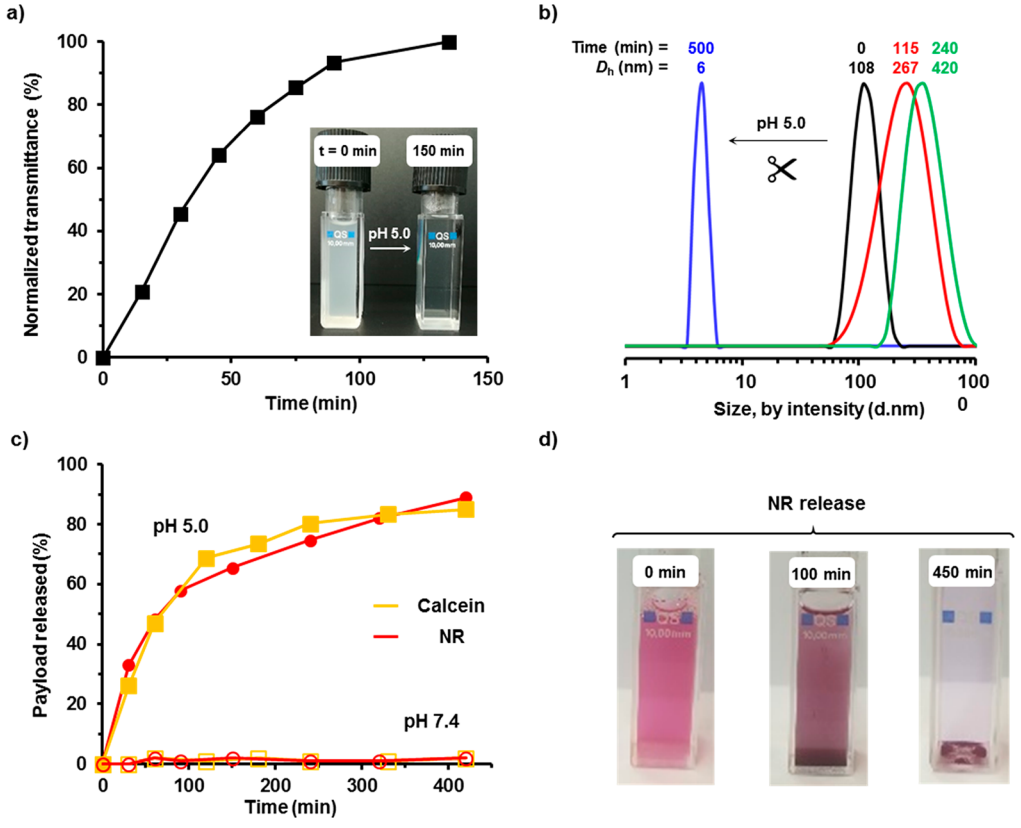

Figure 4. (a) Transmitted laser light intensity evolution vs time for the acidic disassembly of MCCT-POEGA-Br LCMs (20 mg·mL) at pH 5.0. (b) DLS measurements obtained during the acidic disassembly of MCCT-POEGA-Br LCMs (1 mg·mL) at pH 5.0. (c) Calcein and NR release profile from MCCT-POEGA-Br nanoassemblies in aqueous solution at pH 7.4 (close symbols) and 5.0 (open symbols). (d) Digital images captured during the NR release experiment showing the release of the hydrophobic dye in water.

DOI: 10.1021/acsmacrolett.9b00572
ACS Macro Lett. 2019, 8, 1200−1208

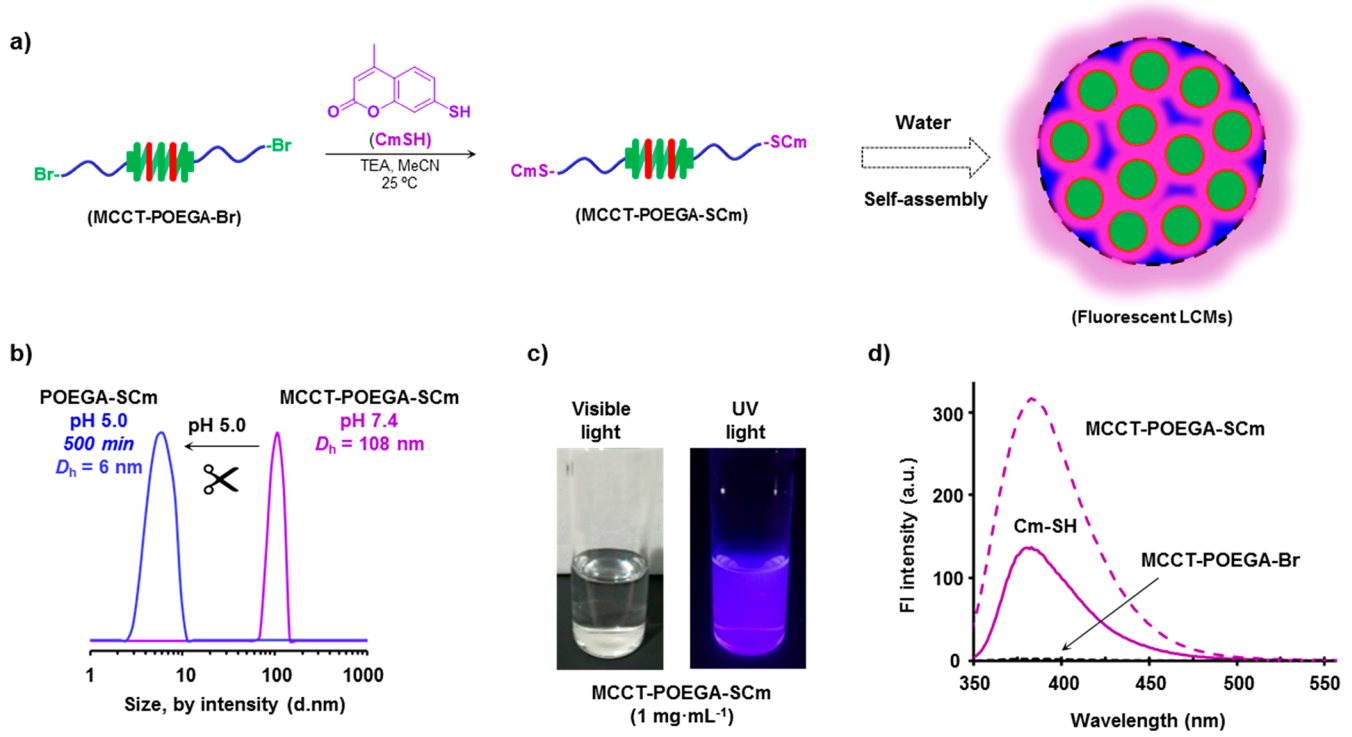

Figure 5. (a) Thio-bromo "click" thioetherification at both polymer end groups of MCCT-POEGA-Br with Cm-SH and subsequent initiator residue-driven micellar assembly in water to obtain fluorescent LCM assemblies. (b) DLS data for fluorescent MCCT-POEGA-SCm assemblies before (purple trace) and after (POEGA-SCm, blue trace) acidic treatment at pH 5.0. (c) Digital images of the MCCT-POEGA-SCm aqueous solution (1 mg·mL^{-1}) irradiated under visible and 365 nm UV light. (d) Fluorescence emission spectra of the THF solutions of MCCT-POEGA-SCm, Cm-SH, and MCCT-POEGA-Br at 1 mg·mL^{-1}.

emission spectrum measured in water (λ_{max} = 507 nm; Figure 3b, dashed yellow line). When the same amount of water-soluble dye was treated with an aqueous solution of MCCT-POEGA-Br (1 mg·mL^{-1}), the resulting dialyzed solution also showed the characteristic emission peak of calcein (yellow line). However, due to the self-quenching properties of this dye, the spectrum of LCM-encapsulated calcein showed much reduced intensity than when the same amount of dye is homogeneously distributed in an aqueous solution.[58]

In this case, the calcein loading content was determined to be slightly lower (5.5%). These results clearly reflect that LCMs self-assembled from MCCT-POEGA-Br can encapsulate both hydrophobic and hydrophilic compounds, thus, being an important advantage when compared with spherical micelles.

In analogy to our recent study,[43] GPC analysis demonstrated that the symmetric architecture and double acetal functionality at the middle-point of MCCT-POEGA-Br allow clear-cut cleavage under acidic conditions to yield two shorter polymeric products (Figure S9). Thus, after demonstrating the reservoir capabilities of the synthesized nanoassemblies, we envisioned a significant change in the amphiphilic character of the constituent telechelic homopolymer in water after middle-chain cleavage. First, we validated this hypothesis via turbidity measurements (Figure 4a). When a turbid aqueous solution of MCCT-POEGA-Br (20 mg·mL^{-1}) was adjusted at pH 5.0, the transmitted laser light progressively increased due to the disruption of nanoassemblies via midchain acid-catalyzed hydrolysis of the parent MCCT-POEGA-Br telechelic polymer. The disassembly process was then also monitored by DLS. As can be seen in Figure 4b, after adjusting the pH value of the solution to 5.0 and increase the incubation time, micellar aggregates were dramatically damaged as reflected by considerable changes of the average D_h. First, MCCT-POEGA-Br assemblies became larger due to degradation-promoted swelling but later declined to D_h = 6 nm after 6.5 h, thus, providing evidence for the proposed disassembly of LCMS into single random coil polymer chains (Scheme 1). Overall, these results support that the folded chain structure of the telechelic polymer is the dominant conformation in LCM nano-assemblies. This important result confirms that MCCT-POEGA-Br assemblies might respond to acidic pH values found in tumor environments or specific intracellular organelles (e.g., endosomes/lysosomes) upon uptake in targeted cells. Next, we examined their potential as responsive nanocarriers for both hydrophobic and hydrophilic guest molecules. NR and calcein were independently loaded into the LCMs, and the pH-triggered release was evaluated at pH 5.0 (Figure 4c). Control experiments (pH 7.4) confirmed that LCM assemblies can preserve the architecture at physiological pH as the fluorescence intensity of both fluorescent dyes remained constant (open symbols). However, upon exposure of the NR-loaded LCMs to acidic pH, a progressive decrease of the pink color of the solution was observed (Figure 4d). Accordingly, fluorescence spectroscopy measurements revealed also a decrease of the fluorescence intensity at 617 nm (Figure S10). This can be reasonably attributed to the release of NR into water due to the disassembly of LCMs via middle-chain cleavage of MCCT-POEGA-Br homopolymer. Approximately 50% of the loaded NR was released in the first 60 min, whereas then this value sharply rose above 90% after approximately 7 h (Figure 4c).

DOI: 10.1021/acsmacrolett.9b00572
ACS Macro Lett. 2019, 8, 1200−1208

Similarly, acidic stimulation also allowed the sustained release of encapsulated hydrophilic calcein in a similar rate (Figure 4d). However, in this case, fluorescence measurements revealed an expected increase of fluorescence intensity during the experiment due to the displacement of the fluorescent probe into the aqueous solution which causes disappearance of self-quenching effect (Figure S11). These experimental results clearly demonstrate that MCCT-POEGA-Br LCMs are effective pH-responsive nanocarriers capable of loading and releasing both hydrophilic and hydrophobic compounds under mimicking biologically relevant acidic environments.

Finally, on account of high bromine chain-end functionality of the synthesized MCCT-POEGA-Br telechelic homopolymer, the preparation of dye-labeled pH-responsive vehicles was also investigated (Figure 5a). First, a blue-fluorescent 7-mercapto-4-methylcoumarin (Cm-SH) dye was anchored at α- and ω-bromo chain ends of MCCT-POEGA-Br using conventional thio-bromo "click" thioetherification reaction conditions. ^{1}H NMR analysis was used to demonstrate the quantitative attachment of the fluorescent probe at both chain ends of the telechelic polymer (Figure 2, upper spectrum). As can be seen in Figure 5b, MCCT-POEGA-SCm also self-assembles into nanoaggregates, with a mean diameter of about 100 nm via direct dissolution of the hydrophilic polymer in water. Indeed, the size of the resulting assemblies dramatically decreased when the pH was decreased from 7.4 to 5.0 due to pH-responsive behavior. Digital images of the self-assembly solution irradiated under visible and 365 nm UV light, together with fluorescence spectroscopy and confocal laser scanning microscopy measurements demonstrated the successful preparation of blue-fluorescent pH-cleavable nanoobjects (Figure 5c,d and S12, respectively). This experiment showcases an effective approach to expand the functional properties of this and other nanoassemblies prepared from hydrophilic telechelic polymers via anchoring or fluorescent tags, drug affinity labels by thio-bromo "click" chemistry, or other efficient transformations.[59]

In conclusion, the simple design strategy based on cleavable difunctional initiators demonstrated here is expected to endow a large diversity of new concepts in supramolecular nanoassemblies with numerous potential technological applications derived from conventional commercial monomers.

■ ASSOCIATED CONTENT

Supporting Information

The Supporting Information is available free of charge on the ACS Publications website at DOI: 10.1021/acsmacrolett.9b00572.

Addition characterization results including materials, experimental procedures, characterization techniques, and additional data (GPC, NMR, DLS, fluorescence spectra, and confocal fluorescence microscopy images (PDF)

■ AUTHOR INFORMATION

Corresponding Authors

*E-mail: percec@sas.upenn.edu.
*E-mail: gerard.lligadas@urv.cat.

ORCID

Marina Galià: 0000-0002-4359-4510
Gerard Lligadas: 0000-0002-8519-1840
Virgil Percec: 0000-0001-5926-0489

Notes

The authors declare no competing financial interest.

■ ACKNOWLEDGMENTS

Financial support from the National Science Foundation Grants DMR-1066116 and DMR-1807127 and the P. Roy Vagelos Chair at the University of Pennsylvania (to V.P.) are gratefully acknowledged. We also thank Spanish Ministerio de Ciencia, Innovación y Universidades through Project MAT2017-82669-R (to G.L. and J.C.R.) and FPI Grant BES-2015-072662 (to A.M.) and the Serra Hunter Programme of the Government of Catalonia (to G.L.). The authors also thank Dr Cesar Rodriguez-Emmenegger for helpful discussions.

■ REFERENCES

(1) Brendel, J. C.; Schacher, F. H. Block Copolymer Self-Assembly in Solution - Quo Vadis? *Chem. - Asian J.* **2018**, *13*, 230−239.
(2) Epps, T. H., III; O'Reilly, R. K. Block Copolymers: Controlling Nanostructure to Generate Functional Materials - Synthesis, Characterization, and Engineering. *Chem. Sci.* **2016**, *7*, 1674−1689.
(3) Wei, M.; Gao, Y.; Li, X.; Serpe, M. J. Stimuli-Responsive Polymers and their Applications. *Polym. Chem.* **2017**, *8*, 127−143.
(4) Bawa, K. K.; Oh, J. K. Stimulus-Responsive Degradable Polylactide-Based Block Copolymer Nanoassemblies for Controlled/Enhanced Drug Delivery. *Mol. Pharmaceutics* **2017**, *14*, 2460−2474.
(5) Mura, S.; Nicolas, J.; Couvreur, P. Stimuli-Responsive Nanocarriers for Drug Delivery. *Nat. Mater.* **2013**, *12*, 991−1003.
(6) Zhang, Q.; Re Ko, N.; Kwon Oh, J. Recent Advances In Stimuli-Responsive Degradable Block Copolymer Micelles: Synthesis And Controlled Drug Delivery Applications. *Chem. Commun.* **2012**, *48*, 7542−7552.
(7) Zhu, A.; Miao, K.; Deng, Y.; Ke, H.; He, H.; Yang, T.; Guo, M.; Li, Y.; Guo, Z.; Wang, Y.; Yang, X.; Zhao, Y.; Chen, H. Dually pH/Reduction-Responsive Vesicles for Ultrahigh-Contrast Fluorescence Imaging and ThermoChemotherapy-Synergized Tumor Ablation. *ACS Nano* **2015**, *9*, 7874−7885.
(8) Patil, N. G.; Basutkar, N. B.; Ambade, A. V. Visible Light-Triggered Disruption of Micelles of an Amphiphilic Block Copolymer with BODIPY at the Junction. *Chem. Commun.* **2015**, *51*, 17708−17711.
(9) Li, Y.; Liu, G.; Wang, X.; Hu, J.; Liu, S. Enzyme-Responsive Polymeric Vesicles for Bacterial-Strain-Selective Delivery of Antimicrobial Agents. *Angew. Chem., Int. Ed.* **2016**, *55*, 1760−1764.
(10) Yan, Q.; Sang, W. H_2S Gasotransmitter-Responsive Polymer Vesicles. *Chem. Sci.* **2016**, *7*, 2100−2105.
(11) Gatenby, R. A.; Gillies, R. J. A Microenvironmental Model of Carcinogenesis. *Nat. Rev. Cancer* **2008**, *8*, 56−61.
(12) Tannock, I. F.; Rotin, D. Acid pH in Tumors and its Potential for Therapeutic Exploitation. *Cancer Res.* **1989**, *49*, 4373−4384.
(13) Murthy, N.; Thng, Y. X.; Schuck, S.; Xu, M. C.; Fréchet, J. M. J. A Novel Strategy for Encapsulation. *J. Am. Chem. Soc.* **2002**, *124*, 12398−12399.
(14) Lin, S.; Du, F.; Wang, Y.; Ji, S.; Liang, D.; Yu, L.; Li, Z. An Acid-Labile Block Copolymer of PDMAEMA and PEG as Potential Carrier for Intelligent Gene Delivery Systems. *Biomacromolecules* **2008**, *9*, 109−115.
(15) Satoh, K.; Poelma, J. E.; Campos, L. M.; Stahl, B.; Hawker, C. J. A Facile Synthesis of Clickable and Acid-Cleavable PEO for Acid-Degradable Block Copolymers. *Polym. Chem.* **2012**, *3*, 1890−1898.
(16) Sedlák, M.; Koňák, C. A New Approach to Polymer Self-assembly into Stable Nanoparticles: Poly(ethylacrylic acid) Homopolymers. *Macromolecules* **2009**, *42*, 7430−7438.
(17) Li, N.; Ye, G.; He, Y.; Wang, X. Hollow Microspheres of Amphiphilic Azo Homopolymers: Self-Assembly and Photoinduced Deformation Behavior. *Chem. Commun.* **2011**, *47*, 4757−4759.

DOI: 10.1021/acsmacrolett.9b00572
ACS Macro Lett. 2019, 8, 1200−1208

(18) Mane, S. R.; Rao N, V.; Chaterjee, K.; Dinda, H.; Nag, S.; Kishore, A.; Das Sarma, J.; Shunmugam, R. Amphiphilic Homopolymer Vesicles as Unique Nano-Carriers for Cancer Therapy. *Macromolecules* **2012**, *45*, 8037−8042.
(19) Zhang, J.; Liu, K.; Müllen, K.; Yin, M. Self-Assemblies of Amphiphilic Homopolymers: Synthesis, Morphology Studies and Biomedical Applications. *Chem. Commun.* **2015**, *51*, 11541−11555.
(20) Savariar, E. N.; Aathimanikandan, S. V.; Thayumanavan, S. Supramolecular Assemblies from Amphiphilic Homopolymers: Testing the Scope. *J. Am. Chem. Soc.* **2006**, *128*, 16224−16230.
(21) Noh, H.; Kim, H. J.; Yang, S. K. Synthesis of Amphiphilic Homopolymers and Their Self-Assembly into Acid-Responsive Polymeric Micelles. *J. Polym. Sci., Part A: Polym. Chem.* **2017**, *55*, 3804−3808.
(22) Ramireddy, R. R.; Prasad, P.; Finne, A.; Thayumanavan, S. Zwitterionic Amphiphilic Homopolymer Assemblies. *Polym. Chem.* **2015**, *6*, 6083−6087.
(23) Mane, S. R.; Rao, N. V.; Shunmugam, R. Reversible pH- and Lipid-Sensitive Vesicles from Amphiphilic Norbornene-Derived Thiobarbiturate Homopolymers. *ACS Macro Lett.* **2012**, *1*, 482−488.
(24) Zhang, J.; You, S.; Yan, S.; Müllen, K.; Yang, W.; Yin, M. pH-Responsive Self-Assembly of Fluorophore-Ended Homopolymers. *Chem. Commun.* **2014**, *50*, 7511−7513.
(25) Wang, Y.; Alb, A. M.; He, J.; Grayson, S. M. Neutral Linear Amphiphilic Homopolymers Prepared by Atom Transfer Radical Polymerization. *Polym. Chem.* **2014**, *5*, 622−629.
(26) Kubo, T.; Easterling, C. P.; Olson, R. A.; Sumerlin, B. S. Synthesis of Multifunctional Homopolymers *via* Sequential Post-Polymerization Reactions. *Polym. Chem.* **2018**, *9*, 4605−4610.
(27) Kubo, T.; Bentz, K. C.; Powell, K. C.; Figg, C. A.; Swartz, J. L.; Tansky, M.; Chauhan, A.; Savin, D. A.; Sumerlin, B. S. Modular and Rapid Access to Amphiphilic Homopolymers via Successive Chemoselective Post-Polymerization Modification. *Polym. Chem.* **2017**, *8*, 6028−6032.
(28) He, H.; Liu, B.; Wang, M.; Vachet, R. W.; Thayumanavan, S. Sequential Nucleophilic "Click" Reactions for Functional Amphiphilic Homopolymers. *Polym. Chem.* **2019**, *10*, 187−193.
(29) Zhou, D.; Gao, Y.; Sigen, A.; Xu, Q.; Meng, Z.; Greiser, U.; Wang, W. Anticancer Drug Disulfiram for In Situ RAFT Polymerization: Controlled Polymerization, Multifacet Self-Assembly, and Efficient Drug Delivery. *ACS Macro Lett.* **2016**, *5*, 1266−1272.
(30) Liu, T.; Tian, W.; Zhu, Y.; Bai, Y.; Yan, H.; Du, J. How Does a Tiny Terminal Alkynyl End Group Drive Fully Hydrophilic Homopolymers to Self-Assemble Into Multicompartment Vesicles and Flower-Like Complex Particles? *Polym. Chem.* **2014**, *5*, 5077−5088.
(31) Patterson, J. P.; Kelley, E. G.; Murphy, R. P.; Moughton, A. O.; Robin, M. P.; Lu, A.; Colombani, O.; Chassenieux, C.; Cheung, D.; Sullivan, M. O.; Epps, T. H., III; O'Reilly, R. K. Structural Characterization of Amphiphilic Homopolymer Micelles Using Light Scattering, SANS, and Cryo-TEM. *Macromolecules* **2013**, *46*, 6319−6325.
(32) Patterson, J. P.; Cotanda, P.; Kelley, E. G.; Moughton, A. O.; Lu, A.; Epps, T. H., III; O'Reilly, R. K. Catalytic Y-Tailed Amphiphilic Homopolymers-Aqueous Nanoreactors for High Activity, Low Loading SCS Pincer Catalysts. *Polym. Chem.* **2013**, *4*, 2033−2039.
(33) Lutz, J. F.; Pfeifer, S.; Zarafshani, Z. In Situ Functionalization of Thermoresponsive Polymeric Micelles using the "Click" Cycloaddition of Azides and Alkynes. *QSAR Comb. Sci.* **2007**, *26*, 1151−1158.
(34) Du, J.; Willcock, H.; Patterson, J. P.; Portman, I.; O'Reilly, R. K. Self-Assembly of Hydrophilic Homopolymers: A Matter of RAFT End Groups. *Small* **2011**, *7*, 2070−2080.
(35) Koga, T.; Tanaka, F.; Motokawa, R.; Koizumi, S.; Winnik, F. M. Theoretical Modeling of Associated Structures in Aqueous Solutions of Hydrophobically Modified Telechelic PNIPAM Based on a Neutron Scattering Study. *Macromolecules* **2008**, *41*, 9413−9422.
(36) Mabire, A. B.; Robin, M. P.; Willcock, H.; Pitto-Barry, A.; Kirby, N.; O'Reilly, R. K. Dual Effect of Thiol Addition on Fluorescent Polymeric Micelles: ON-to-OFF Emissive Switch and Morphology Transition. *Chem. Commun.* **2014**, *50*, 11492−11495.
(37) Nguyen, N. H.; Kulis, J.; Sun, H. J.; Jia, Z.; van Beusekom, B.; Levere, M. E.; Wilson, D. A.; Monteiro, M. J.; Percec, V. A Comparative Study of the SET-LRP of Oligo(ethylene oxide) Methyl Ether Acrylate in DMSO and in H_2O. *Polym. Chem.* **2013**, *4*, 144−155.
(38) Percec, V.; Guliashvili, T.; Ladislaw, J. S.; Wistrand, A.; Stjerndahl, A.; Sienkowska, M. J.; Monteiro, M. J.; Sahoo, S. Ultrafast Synthesis of Ultrahigh Molar Mass Polymers by Metal-Catalyzed Living Radical Polymerization of Acrylates, Methacrylates, and Vinyl Chloride Mediated by SET at 25 °C. *J. Am. Chem. Soc.* **2006**, *128*, 14156−14165.
(39) Percec, V.; Popov, A. V.; Ramirez-Castillo, E.; Monteiro, M.; Barboiu, B.; Weichold, O.; Asandei, A. D.; Mitchell, C. M. Aqueous Room Temperature Metal-Catalyzed Radical Polymerization of Vinyl Chloride. *J. Am. Chem. Soc.* **2002**, *124*, 4940−4941.
(40) Rosen, B. M.; Percec, V. Single-Electron Transfer and Single-Electron Transfer Degenerative Chain Transfer Living Radical Polymerization. *Chem. Rev.* **2009**, *109*, 5069−5119.
(41) Zhang, N.; Samanta, S. R.; Rosen, B. M.; Percec, V. Single Electron Transfer in Radical Ion and Radical-Mediated Organic, Materials and Polymer Synthesis. *Chem. Rev.* **2014**, *114*, 5848−5958.
(42) Lligadas, G.; Grama, S.; Percec, V. Single-Electron Transfer Living Radical Polymerization Platform to Practice, Develop and Invent. *Biomacromolecules* **2017**, *18*, 2981−3008.
(43) Moreno, A.; Ronda, J. C.; Cádiz, V.; Galià, M.; Lligadas, G.; Percec, V. SET-LRP from Programmed Difunctional Initiators Encoded with Double Single-Cleavage and Double Dual-Cleavage Groups. *Biomacromolecules* **2019**, *20*, 3200−3210.
(44) Zhang, S.; Xiao, Q.; Sherman, S. E.; Muncan, A.; Ramos Vicente, A. D. M.; Wang, Z.; Hammer, D. A.; Williams, D.; Chen, Y.; Pochan, D. J.; Vértesy, S.; André, S.; Klein, M. L.; Gabius, H. J.; Percec, V. Glycodendrimersomes from Sequence-Defined Janus Glycodendrimers Reveal High Activity and Sensor Capacity for the Agglutination by Natural Variants of Human Lectins. *J. Am. Chem. Soc.* **2015**, *137*, 13334−13344.
(45) Xiao, Q.; Zhang, S.; Wang, Z.; Sherman, S. E.; Moussodia, R. O.; Peterca, M.; Muncan, A.; Williams, D. R.; Hammer, D. A.; Vértesy, S.; André, S.; Gabius, H. J.; Klein, M. L.; Percec, V. Onion-like Glycodendrimersomes from Sequence-Defined Janus Glycodendrimers and Influence of Architecture on Reactivity to a Lectin. *Proc. Natl. Acad. Sci. U. S. A.* **2016**, *113*, 1162−1167.
(46) Rodriguez-Emmenegger, C.; Xiao, Q.; Kostina, N. Y.; Sherman, S. E.; Rahimi, K.; Partridge, B. E.; Li, S.; Sahoo, D.; Reveron Perez, A. M.; Buzzacchera, I.; Han, H.; Kerzner, M.; Malhotra, I.; Möller, M.; Wilson, C. J.; Good, M. C.; Goulian, M.; Baumgart, T.; Klein, M. L.; Percec, V. Encoding Biological Recognition in a Bicomponent Cell-Membrane Mimic. *Proc. Natl. Acad. Sci. U. S. A.* **2019**, *116*, 5376−5382.
(47) Rosen, B. M.; Lligadas, G.; Hahn, C.; Percec, V. Synthesis of Dendrimers Through Divergent Iterative Thio-Bromo "Click" Chemistry. *J. Polym. Sci., Part A: Polym. Chem.* **2009**, *47*, 3931−3939.
(48) Rosen, B. M.; Lligadas, G.; Hahn, C.; Percec, V. Synthesis of Dendritic Macromolecules Through Divergent Iterative Thio-Bromo "Click" Chemistry and SET-LRP. *J. Polym. Sci., Part A: Polym. Chem.* **2009**, *47*, 3940−3948.
(49) Soeriyadi, A. H.; Boyer, C.; Nyström, F.; Zetterlund, P. B.; Whittaker, M. R. High-Order Multiblock Copolymers via Iterative Cu(0)-Mediated Radical Polymerizations (SET-LRP): Toward Biological Precision. *J. Am. Chem. Soc.* **2011**, *133*, 11128−11131.
(50) Nguyen, N. H.; Levere, M. E.; Percec, V. SET-LRP of Methyl Acrylate to Complete Conversion with Zero Termination. *J. Polym. Sci., Part A: Polym. Chem.* **2012**, *50*, 860−873.
(51) Beyer, V. P.; Cattoz, B.; Strong, A.; Phillips, D. J.; Schwarz, A.; Becer, C. R. Fast Track Access to Multi-block Copolymers via Thiol-Bromo Click Reaction of Telechelic Dibromo Polymers. *Polym. Chem.* **2019**, *10*, 4259−4270.

DOI: 10.1021/acsmacrolett.9b00572
ACS Macro Lett. 2019, 8, 1200−1208

(52) Bao, C.; Yin, Y.; Zhang, Q. Synthesis and Assembly of Laccase-Polymer Giant Amphiphiles by Self-Catalyzed CuAAC Click Chemistry. *Biomacromolecules* **2018**, *19*, 1539−1551.
(53) Simula, A.; Nurumbetov, G.; Anastasaki, A.; Wilson, P.; Haddleton, D. M. Synthesis and Reactivity of α,ω-Homotelechelic Polymers by Cu(0)-mediated Living Radical Polymerization. *Eur. Polym. J.* **2015**, *62*, 294−303.
(54) Zhang, L.; Eisenberg, A. Multiple Morphologies and Characteristics of "Crew-Cut" Micelle-like Aggregates of Polystyrene-b-poly(acrylic acid) Diblock Copolymers in Aqueous Solutions. *J. Am. Chem. Soc.* **1996**, *118*, 3168−3181.
(55) Feng, C.; Lu, G.; Li, Y.; Huang, X. Self-Assembly of Amphiphilic Homopolymers Bearing Ferrocene and Carboxyl Functionalities: Effect of Polymer Concentration, β-Cyclodextrin, and Length of Alkyl Linker. *Langmuir* **2013**, *29*, 10922−10931.
(56) Xu, B.; Gu, G.; Feng, C.; Jiang, X.; Hu, J.; Lu, G.; Zhang, S.; Huang, X. (PAA-*g*-PS)-*co*-PPEGMEMA Asymmetric Polymer Brushes: Synthesis, Self-Assembly, and Encapsulating Capacity for Both Hydrophobic and Hydrophilic Agents. *Polym. Chem.* **2016**, *7*, 613−624.
(57) Zhu, J. L.; Liu, K. L.; Zhang, Z.; Zhang, X. Z.; Li, J. Amphiphilic Star-Block Copolymers and Supramolecular Transformations of Nanogel-Like Micelles to Nanovesicles. *Chem. Commun.* **2011**, *47*, 12849−12851.
(58) Mondal, T.; Dan, K.; Deb, J.; Jana, S. S.; Ghosh, S. Hydrogen-Bonding-Induced Chain Folding and Vesicular Assembly of an Amphiphilic Polyurethane. *Langmuir* **2013**, *29*, 6746−6753.
(59) Anastasaki, A.; Willenbacher, J.; Fleischmann, C.; Gutekunst, W. R.; Hawker, C. J. End Group Modification of Poly(acrylates) Obtained via ATRP: a User Guide. *Polym. Chem.* **2017**, *8*, 689−697.

DOI: 10.1021/acsmacrolett.9b00572
ACS Macro Lett. 2019, 8, 1200−1208